



Dual Targeting of HER-2 and VEGFR-2 Receptors in Breast Cancer-Associated Migration and Metastasis

Masoom Raza *, Naveen Kumar, and Seema Sehrawat

Department of Life Sciences, School of Natural Sciences, Shiv Nadar University, Greater Noida 201314, India

* Correspondence: mr126@snu.edu.in

Received: 2 February 2026; Revised: 18 May 2026; Accepted: 15 June 2026; Published: 30 June 2026

Abstract: There are various types and subtypes of breast cancer cells. One of the most aggressive forms is TNBC, which is characterised by the absence of common hormonal receptors such as HER-2, PR, and ER on the cancer cells. These cancers are difficult to treat, and there is an unmet need for innovative strategies to develop drug combinations that effectively target and cure them. Therefore, we adopted a precision medicine approach to treat TNBC. In this study, we used a combination of two different drugs, Lapatinib and Telatinib, which specifically inhibit tyrosine kinases. We determined the IC₅₀ values for these drugs despite the lack of HER2 receptor expression in MDA-MB-231 cells. Cells treated with these drugs, both individually and together, showed reduced invadopodia formation and decreased cell proliferation. We also observed a significant decrease in 2D angiogenesis tube formation after treatment with these inhibitors. Our data reveal an interesting mechanism of action for Lapatinib and Telatinib in TNBC cells. Collectively, these findings provide preclinical evidence supporting further investigation of HER-2/VEGFR-2 dual targeting as a therapeutic strategy.

Keywords: metastasis; triple negative breast cancer (TNBC); combination therapy; angiogenesis; human cell stress array

1. Introduction

Despite advances in cancer treatments, breast cancer continues to be the leading cause of death among women worldwide, followed by lung cancer [1,2] and ranks as the fourth leading cause of cancer-related death [3]. Breast cancer is a highly heterogeneous disease characterised by substantial variation in tumour biology, genetics, and clinical behaviour, and this diversity significantly influences prognosis and informs personalised treatment strategies. In 2024, an estimated 310,720 new invasive breast cancers and 56,500 cases of ductal carcinoma *in situ* were diagnosed among women in the US. Approximately 1 in 8 women in the US (13.1%) are diagnosed with invasive breast cancer. Breast cancer incidence increased by 1% annually over the most recent decade (2012–2021) [4]. Pathogenic variants in BRCA1 and BRCA2 are associated with markedly increased lifetime risks of breast cancer, estimated at approximately 65–72% for BRCA1 and 60–69% for BRCA2 mutation carriers, compared with ~12–13% in the general population [5–8]. While these estimates are supported by large cohort studies and meta-analyses, variability across studies suggests that additional modifiers, including metabolic and microenvironmental factors, may influence disease penetrance. Emerging evidence indicates that BRCA1/2-associated tumours exhibit distinct metabolic adaptations and mitochondrial alterations that can shape tumour progression and immune responses. These features highlight a potential link between hereditary genomic instability and immunometabolic reprogramming, with important implications for targeted therapeutic strategies. Numerous technologies, such as whole-genome sequencing and functional diagnostics, have helped identify and analyse tumours. Breast tumours can be classified by histological subtype and grade, where grade indicates the degree of differentiation and subtype refers to the tumour growth pattern. The most common breast carcinoma is invasive ductal carcinoma [9]. Breast cancer is not a single disease but a heterogeneous group of malignancies that can be classified by both clinical type and molecular subtype. Broadly, breast cancers may be non-invasive or invasive, and invasive tumours can be further categorized into the molecular subtypes luminal A, luminal B, HER2-enriched, and triple-negative/basal-like. These subtypes differ in receptor status, gene-expression patterns, prognosis, and response to therapy, with luminal A generally being the most common and usually the most favourable subtype (accounts for approximately 50% to 60% of cases), while luminal B (about 15% to 20%),



HER2-enriched (about 10% to 15%), and triple-negative/basal-like tumours (about 10% to 15%) tend to be more aggressive or biologically distinct [10].

The primary treatment for breast cancer, like other solid tumours, remains surgery. Surgical removal can be either a lumpectomy, which removes only the cancerous area, or a mastectomy, which involves removing the entire breast. The choice depends on the cancer's size and location, the breast size, and the patient's preferences [11]. Chemotherapeutic agents like anthracyclines (doxorubicin), taxanes (paclitaxel), 5-fluorouracil, and others are used either to shrink tumours for easier surgical removal or to eliminate remaining cancer cells after surgery [12]. Targeted therapies for breast cancer that inhibit expressed receptor tyrosine kinases are also used based on the cancer cells' expression profile. Several therapeutics targeting HER2/neu are approved for HER2+ breast cancer, such as Trastuzumab and Lapatinib. Poly-(ADP ribose)-polymerase (PARP), which is involved in DNA repair, is also targeted with inhibitors like Olaparib for tumours with BRCA mutations, which already have a defective DNA repair machinery [13]. For tumours overexpressing hormone receptors such as Estrogen/Progesterone (ER/PR), hormone therapy can be used to either block the production of these hormones (such as Anastrozole), block the hormone receptors (such as Tamoxifen), or block ovarian function altogether through oophorectomy or therapeutics such as luteinizing hormone-releasing hormone analogues (such as Leuprolide) and certain chemotherapeutics [13]. For Triple Negative Breast Cancer (TNBC), which does not express HER2 or hormone receptors, chemotherapy remains the main treatment.

Immunotherapy is an appealing option that enhances the immune response through PD-L1 inhibition, such as with therapeutics like Atezolizumab, which is currently used for triple-negative breast cancer. Precision medicine is an approach to prevention, diagnosis, and treatment of disease that considers individual differences in factors like genes, lifestyle, and environment, aiming to offer personalised treatment tailored to each patient [14].

While monotherapy is effective in the short term, it has a drawback: drug resistance in cancer cells develops easily. Combination therapies can overcome this, as multiple drugs can act synergistically to eliminate cancer cells. It has also been observed that combination therapies can reduce the development of resistance and re-sensitize resistant cells [15–17]. Combination therapy is also a way to counter tumour heterogeneity; paclitaxel and salinomycin target rapidly dividing tumour cells and cancer stem cells simultaneously [18]. Chemotherapy for breast cancer is usually given in combination with two or three drugs to damage the cells in more than one way, as well as prevent the development of resistance [12]. Targeted therapeutics are often used in combination with chemotherapy or other targeted agents; HER2 inhibitors combined with chemotherapeutics are the standard of care for HER-2+ breast cancer [17–19], and combination regimens with other inhibitors, such as Pertuzumab, are also in use [13].

Precision medicine refers to customised medical treatment that uses new diagnostics and therapeutics based on a patient's genetic profile. Advances in cell sorting, epigenetics, proteomics, metabolomics, and related fields are converging with informatics and other technologies, rapidly expanding the scope of this field. Antibody conjugated drug Trastuzumab emtansine (T-DM1) combines the specificity of Trastuzumab with cytotoxicity caused by DM1 and is an approved therapeutic for HER2+ breast cancer [19].

We investigated the therapeutic potential of a novel combination of inhibitory small molecules in TNBCs. In this study, we assessed whether a novel combination of inhibitory small molecules, Lapatinib and Telatinib, could suppress TNBC progression, migration, and metastasis. Lapatinib targets EGFR (Epidermal Growth Factor Receptor) and HER2 in breast cancer cells, but in TNBC, it targets only EGFR. Telatinib targets VEGFR-2 & -3 (Vascular Endothelial Growth Factor Receptor-2 & -3) in the tumour microenvironment. Both molecules effectively reduced cell survival in TNBC tumour cells. A combination of Lapatinib and Telatinib inhibits cellular invasive properties and affects the tumour-induced angiogenesis.

The concept of precision medicine has gained importance in the field of breast cancer, but due to the lack of evidence of these driver mutations, very little evidence exists that suggests that it could improve patient outcomes. Thus, the focus should be on identifying these driver mutations, classifying the genes associated with them, and elucidating the pathways activated in cancers. These drivers are the ones that are responsible for the progression of cancer. This information will eventually guide us to develop new combination therapies and improve patient outcomes and survival [20].

2. Materials and Methods

2.1. Antibodies and Reagents

Lapatinib (Cat no. A8218-25 mg, APExBIO, Houston, TX, USA), Telatinib/BAY 57-9352 (Cat no. A8550-5 mg, APExBIO, USA), FITC Annexin V (Ref no. 51-65874, Becton Dickinson, Franklin Lakes, NJ, USA), Propidium Iodide (1 mg/mL, Ref no. P3566, Life Technology, Carlsbad, CA, USA), Alexa Fluor® 555 Phalloidin

(Ref no. 8953, Cell signal, Boston, MA, USA), JC-1; CBIC2 (Ref no. T3168, Molecular probe, Life Technology, USA), ProLong™ Gold antifade reagent with DAPI (Ref no. P36935, Invitrogen by Thermo Fisher Scientific, Waltham, MA, USA), Dulbecco's Phosphate Buffered Saline w/o Calcium, Magnesium and Phenol red 9.6 g/L (Ref no. TS1006, HiMEDIA, Thane, India), Gelatin from Pig skin, Oregon green™ 488 conjugated (Ref no. G13186, Invitrogen, Carlsbad, CA, USA), Human CD 24 FITC conjugated (Ref no. MHCD24014, Life Technology, USA), ADAMTS1 (Cat no. PAB973Hu01), CEACAM1 (Cat no. PAC977Hu01), β -actin (Cat no. PAB340Mi01), MMP2 (Cat no. PAA100Hu01), MMP9 (Cat no. PAA553Hu01), β -catenin (Cat no. PAB021Hu01), PECAM1 (Cat no. PAA363Hu01), VEGFR-2 (Cat no. PAB367Hu01), GAPDH (Cat no. PAB932Hu01), HIF 1 α (Cat no. PAA798Hu01), all antibodies were purchased from Cloud-Clone Corp., Katy, TX, USA. MENA (Cat no. NBP1-87914, Novus, 1:1000), α -tubulin (DM1A, Cat no. NB100-690, Novus, 1:5000), Cell culture inserts (Cat no. MCEP12H48, Millipore), Matrigel (Cat no. 356237, BD Biosciences, San Jose, CA, USA), and 2-mercaptoethanol were purchased from Sigma-Aldrich, USA. Secondary antibody anti-mouse (Cat no. 554002, BD, 1:2000) and anti-rabbit HRP conjugated (Cat no. 554021, BD, 1:2000), Proteome Profiler Human Cell Stress Array Kit (Cat no. ARY018, R&D System, Minneapolis, MN, USA) were obtained. Hypotonic PI solution (5 mg Propidium Iodide, 100 mL MQ, 100 mg Sodium Citrate, 4 mg RNase, 30 μ L Tween-20)

2.2. Cell Culture

MDA-MB-231 cell line was cultured in L-15 (Leibovitz's-15) medium procured from HiMEDIA, India (Ref no. AL011S) and supplemented with 10% FBS (Fetal Bovine Serum, Gibco, Grand Island, NY, USA), 1% Antibiotic antimycotic solution 100X (Ref no. A002A-100 mL, HiMEDIA, India). Subculturing of cells was performed using a 1X trypsin-EDTA solution (Ref no. TCL007-100 mL, HiMEDIA, India). All cell culture experiments were performed in a humidified CO₂ incubator at 37 °C with 5% CO₂.

2.3. Cell Cytotoxicity/Counting Assay

The MDA-MB-231 cell line was sub-cultured with trypsin and seeded into a new 24-well plate at a density of 20,000 cells per well. After 24 h, cells were treated with Lapatinib and Telatinib at concentrations ranging from 1 μ M to 30 μ M. After 72 h of treatment, cells were harvested and counted using a hemocytometer to assess cell survival or cytotoxicity. We obtained IC₅₀ values of approximately 5 μ M for each drug. The rest of the experiment was conducted at this concentration only.

2.4. Wound Healing Assay

MDA-MB-231 cells were harvested and seeded into a new 12-well plate at a density of 0.5×10^5 cells per well. After 24 h, when the cells had reached 60–70% confluency, a linear scratch was created through the monolayer using a sterile 10 μ L pipette tip guided by a ruler. The cell monolayer was then gently washed with phosphate-buffered saline (PBS) to remove detached cells and debris. Lapatinib and Telatinib, prepared in culture medium at concentrations corresponding to their respective IC₅₀ values, were added to the cells individually and in combination. The wound area was monitored for 24 h post-treatment, and images were captured at the indicated time points. The remaining wound area was measured and quantified using ImageJ software v1.5, and wound closure was calculated based on the change in the affected area over time. Percentage wound closure = [(initial wound width-wound width 24 h after treatment with all drugs/control)/initial wound width] \times 100. The resulting data were presented as bar graphs generated using GraphPad Prism software version v8.4.

2.5. Cell Cycle Analysis

Cell cycle analysis was conducted following the previously described protocol [21]. Briefly, MDA-MB-231 cells were harvested and seeded into a 60 mm dish. After 48 h of treatment with Lapatinib and Telatinib at each drug's IC₅₀, cells were washed with 1X PBS. A hypotonic PI solution, already prepared in MQ, was added to the dish and incubated for 20–30 min. All the cells were collected, spun down to form a nuclear pellet, and the pellet was resuspended in hypotonic PI solution. Flow cytometry analysis was performed at an excitation wavelength of 488 nm with broad emission centered at 600 nm. Data were analysed using FlowJo software v10.4.0 (FlowJo, LLC, Ashland, OR, USA).

2.6. Mitochondrial Membrane Potential Assay

Mitochondrial potential was analysed as previously described [22]. Briefly, MDA-MB-231 cells were harvested and seeded into a 60 mm dish. After 48 h of treatment with Lapatinib and Telatinib, according to each

drug's IC₅₀ value, cells were washed with 1X PBS, and a working concentration of 2 µM/mL JC-1 dye (7.7 mM stock in DMSO) was added to each dish prepared in complete cell culture medium for 20–30 min in the dark. Cells were trypsinized and pelleted. The cells were washed with 1X PBS + 0.1% FBS solution and resuspended in PBS with FBS. Flow cytometry analysis was performed on a BD FACSCanto II using 488 nm excitation with 530 nm and 580 nm bandpass emission filters. Data were analysed using FlowJo software v10.4.0 (FlowJo, LLC, Ashland, OR, USA).

2.7. Immunofluorescence Assay

An immunofluorescence assay was performed as previously described [23]. Briefly, MDA-MB-231 cells were seeded onto a glass coverslip in a 12-well plate (approximately 2.0×10^5 cells per well) in 1 mL of complete medium. After 24 h, cells were treated with Lapatinib and Telatinib, diluted separately and in combination, in complete media. Following 24 h, cells were washed twice with ice-cold 1X PBS and fixed with 4% paraformaldehyde for 10 min at room temperature. Cells were permeabilized with 0.1% Triton X-100 (Cat no. X-100-100mL, Millipore Sigma, Milwaukee, WI, USA) in PBS for 10 min at room temperature. Blocking was performed using FBS-PBS (1% FBS) for 2 h at room temperature. Immunostaining involved incubating cells overnight at 4 °C with primary antibodies such as MENA, β-actin, or α-tubulin, followed by a 2-hour incubation with their respective secondary antibodies. Coverslips were mounted using Vector Shield mounting reagent with DAPI and sealed. Slides were examined under an Epifluorescence microscope (Eclipse Ti, Nikon, Melville, NY, USA) and a Confocal Microscope (Nikon Ti2 Eclipse).

2.8. Annexin/PI Assay

Annexin V and PI staining was performed as previously described [24,25]. Briefly, MDA-MB-231 cells were seeded and treated with Lapatinib and Telatinib for 48 h. The cells were harvested with trypsin, pelleted in an Eppendorf tube, and resuspended in 1X PBS. The cells were centrifuged again, and the pellet was resuspended in 1xAnnexin binding buffer. After centrifugation to pellet the cells, 100 µL of 1X Annexin binding buffer was added. Annexin V (1:100) and PI (1:100) were added, and the cells were incubated for 20–30 min in the dark. Subsequently, 500 µL of binding buffer was added for washing. The cells were resuspended in buffer and fixed with 1% formaldehyde solution prepared in Annexin buffer for 10 min on ice. The cells were washed with Annexin buffer and resuspended in the same buffer. Flow cytometry was performed on a BD FACS Canto II using the following excitation/emission (nm) settings: FITC, 494/518; PI, 535/617. Data were analysed using FlowJo software v10.4.0 (FlowJo, LLC, Ashland, OR, USA).

2.9. Invadopodia Assay

MDA-MB-231 cells were harvested and seeded into a 60 mm dish for the Invadopodia experiment. The cells were treated with Lapatinib and Telatinib inhibitors for 48 h. Fluorescent gelatin-coated coverslips were prepared according to the protocol [23,26]. Briefly, cells were harvested with trypsin, the pellet was collected, and the cells were resuspended in complete medium. Then, 20,000 to 40,000 cells were plated onto each gelatin-coated coverslip and incubated for 10–16 h. After incubation, the plates containing the coverslips were washed with PBS and quickly fixed in 4% formaldehyde for 10–15 min at room temperature. The fixation solution was then removed, and the coverslips were washed twice with PBS. They were then incubated in a BSA solution (3% BSA in PBS containing 0.1% Triton X-100) for 15–20 min at room temperature in the dark. Following this, the BSA solution was removed, and the coverslips were washed twice with PBS. The coverslips were stained with Alexa Fluor 555 Phalloidin (1:500 dilution) for 30–40 min in the dark. After staining, the coverslips were washed twice with PBS, then mounted by inverting them onto a glass slide with a drop of ProLong™ Gold antifade reagent containing DAPI. The mounted samples were left to dry, the coverslips were sealed, and the samples were stored at 4 °C. Images were taken using a fluorescent microscope.

2.10. Angiogenesis Assay

Angiogenesis, tubes/branches, and node formation were performed as previously described [23]. Briefly, HUVECs (Human Umbilical Vein Endothelial Cells) (approximately 5.0×10^3 cells/well) were seeded onto a Matrigel (10 mg/mL)-coated 96-well plate in EBM media. First, Matrigel was thawed at 4 °C, and 100 µL of Matrigel was coated in each well. The plate was then incubated at 37 °C for 30 min. Primary cells were harvested, and an equal number of cells was seeded on top of the Matrigel with an equal concentration of TCM from the control and all drug-treated MDA-MB-231 and MDA-MB-453 cells. Cells were incubated at 37 °C, 5% CO₂. The

images were taken after 4, 8, and 12 h, and the nodes and branches were carefully analysed from each well using AngioTool v0.6a. Branches and nodes were counted, and graphs were created using GraphPad Prism v8.4.

2.11. Western Blotting

Western blot analysis was conducted as previously described [23]. Briefly, TNBCs were plated in a culture dish, and after 24 h, treated with the IC₅₀ values of each drug, Lapatinib and Telatinib, for an additional 24 h. Cells were then harvested, resuspended in RIPA buffer, and evenly distributed. Total protein was quantified and loaded at equal concentrations onto an SDS-PAGE gel for 3–4 h. Proteins were transferred to a nitrocellulose membrane for blotting. Western blotting was performed using antibodies against VEGFR-2, EGFR, PECAM1, CEACAM1, ADAMTS1, HIF-1 α , β -catenin, Occludin, TGF- β 1, E-cadherin, GM-130, NF κ -B1, MMP2, and MMP9. The blots were developed with Bio-Rad ECL solutions, and the images were quantified using ImageJ. Graphs were generated with GraphPad Prism 8.4.

2.12. Proteome Profiler Human Cell Stress Array Analysis

Stress array was conducted according to our previously published paper [23]. Briefly, MDA-MB-231 cells were seeded in a Petri dish and then treated with the combination of Lapatinib and Telatinib for 24 h. Total cell lysates were collected and stored at –80 °C. The total protein concentration was determined using the Bradford method and added to each membrane of the stress array for overnight incubation. The next step followed the manufacturer's protocol provided with the array kit. The array blot was quantified using ImageJ software v1.5, and the graphs were generated with GraphPad Prism v8.4.

2.13. Statistical Analysis

We analysed our data using GraphPad Prism version 8.4. Cell survival (50% cell death) was determined using a cell counting assay, and the data were used to plot the graph. Western blot membrane quantification for all proteins was performed using ImageJ, and the mean and standard deviation were calculated. Graphs were created using a two-way ANOVA test. Angiogenesis nodes and branches were counted and analysed, with the mean and standard deviation calculated using an unpaired t-test. Graphs were generated accordingly. Significance was considered at a P value less than 0.05.

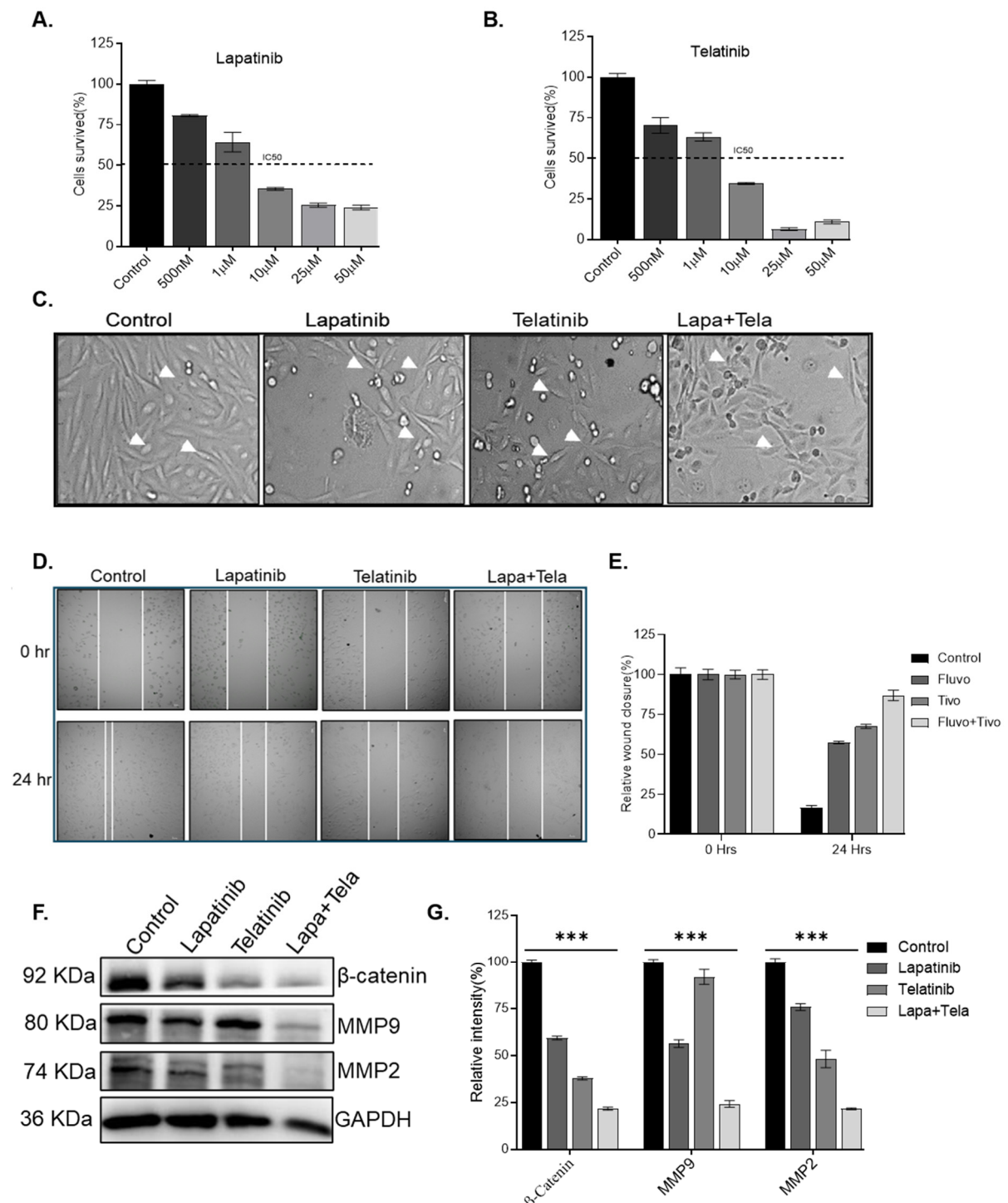
3. Results

3.1. The Synergistic Effect of Lapatinib and Telatinib Affects the Cellular Morphology and Inhibits the Migration of Cancer Cells

We first evaluated the cell survival potential of MDA-MB-231 and MDA-MB-453 cells after treatment with Lapatinib and Telatinib. Cells were exposed for 48 h, followed by both morphological and quantitative assessments. While Lapatinib is effective in HER2-positive cells by disrupting the HER2 pathway, we observed a significant survival benefit even in HER2-negative cells. The cell survival assay revealed a wide range of inhibitory molecules, with IC₅₀ values of 5 μ M for both compounds (Figure 1A,B,H). The effect of Telatinib was also apparent in cellular morphology. We then treated the cells with a combination of Lapatinib and Telatinib and observed that their cellular morphology was markedly different from that of control cells. Both cell types shrank and became round after treatment with both drugs. Individual treatments caused noticeable changes in cellular structures, indicating that Lapatinib and Telatinib influence cellular functions and behaviours that deserve further study (Figure 1C,I).

Cancer cell migration is a hallmark of cancer progression. We aimed to understand cellular motility while targeting specific molecules in combination. During this combined treatment, we found that our novel combination molecules are highly effective at inhibiting cellular motility. A combination of Lapatinib and Telatinib significantly reduced cell migration compared to control cells (Figure 1D,E). To better understand the roles of molecular players in cancer cell migration, we examined the protein expression of key molecules involved in metastasis. β -catenin, a pivotal factor in cancer progression and EMT, was found to be decreased with the combination treatment (Figure 1F). It is reported that nuclear accumulation of β -catenin and its target cyclin D1 is linked to worse outcomes in breast cancer patients. β -catenin interacts with DNA-binding proteins, thereby increasing cyclin D1 and c-Myc levels, which support tumour progression and motility [27–29]. The degradation of the extracellular matrix (ECM) is a crucial step in tumour metastasis. Among the various protein families involved in this process, zinc-dependent matrix metalloproteinases (MMPs) play a leading role in ECM degradation observed in several diseases [30,31]. Studies on various subtypes of breast cancer suggest an increase

in the expression of MMP2 and MMP9, which is associated with a poorer prognosis [32]. MMP9 can degrade collagen and therefore contributes to basement membrane degeneration, supporting tumour invasion and metastasis. Several *in vitro* and *in vivo* studies using cancer models have shown that MMP9 upregulation correlates with tumour progression [33]. Consequently, MMP9 expression is significantly increased in more aggressive breast cancers, including TNBC [34]. Among the various MMPs, MMP2 is involved in breaking through the basement membrane and is thus highly concentrated in tumours prone to metastasis. It is believed to contribute to breast cancer invasion and spread. This is supported by various *in vitro* and *in vivo* data demonstrating that increased MMP2 drives tumour progression. [35,36]. As with β -catenin, our findings showed that a combination of drugs significantly affected MMP2 and 9 protein levels, as shown by Western blots (Figure 1F,G). MMP2 and MMP9 are the primary proteases involved in breast cancer cell migration. MMPs are matrix metalloproteases that regulate the extracellular matrix. Inhibiting MMP2 and MMP9 alongside our compounds supports our previous data on cell migration inhibition. Since ECM degradation was reduced, cancer cells lost their ability to move further.



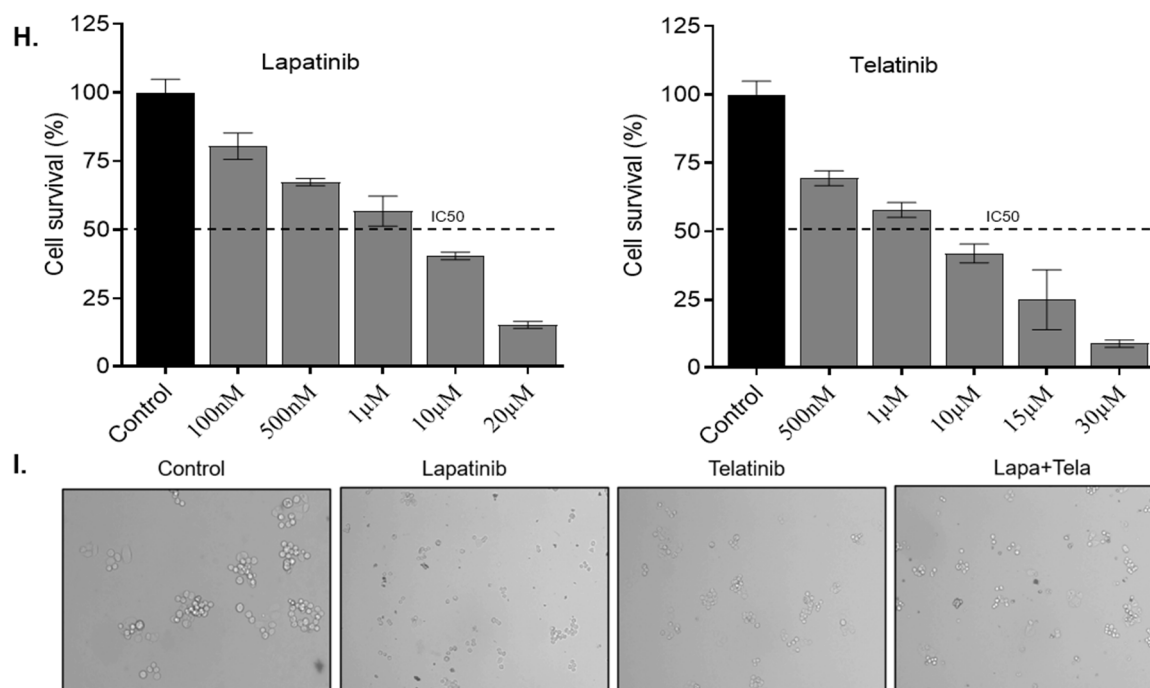


Figure 1. Cytotoxicity of MDA-MB-231 cells after treatment with Lapatinib and Telatinib. (AB) MDA-MB-231 cells (2×10^4 cells/well) were seeded in a 24-well plate, allowed to adhere for 10 h, and then treated with various concentrations of Lapatinib and Telatinib, ranging from 500 nM to 50 μ M, for 72 h. Afterwards, cells were harvested and counted with a hemocytometer. The bar graphs showed the IC₅₀ values for each drug, generated using GraphPad Prism. The calculated IC₅₀ values for Lapatinib and Telatinib are both 5 μ M. (C) The morphological analysis of breast cancer cells was observed. After 24 h of treatment, images were captured with an epifluorescence microscope. The control cells appeared elongated, whereas the combination-treated cells looked shrunken and round, indicating apoptosis. (D) MDA-MB-231 cells were seeded in a 12-well plate to assess their wound-healing capacity. A scratch was created using a micropipette tip, then both drugs were added at concentrations based on the IC₅₀ values. The cells were observed over the next 24 h, and the scratch was analysed using ImageJ software v1.5. Cell migration was reduced in the combination-treated group compared with the control. (E) The bar graph compares the wound area at 0 h and 24 h. After 24 h, the wound area in the combination-treated group was nearly the same as at 0 h, indicating impaired migration of breast cancer cells. (F,G) Western blot analysis was performed for the following molecules: β -catenin, MMP2, and MMP9, which are key proteins involved in cancer cell migration and metastasis. The data indicated that breast cancer cells showed lower expression of these molecules in the combination-treated group than in the control group. (H,I) Lapatinib and Telatinib IC₅₀ values were calculated in another breast cancer cell line, MDA-MB-453 and cytotoxicity assays were determined. Cell morphologies were presented. The graphs were made using GraphPad Prism software v8.4. Values are shown as mean \pm SEM. Statistical significance was determined using two-way ANOVA (factors: treatment group and time point) for Figure 1E; 1-way ANOVA was used to determine statistical significance for the remaining graphs. *** $p < 0.001$.

3.2. Membrane Potential and Cell Cycle Remain Unaffected after the Treatment with Inhibitors

Cell survival and morphological assays indicated cellular stress, which we analysed using PI and JC1 staining. Treatment with inhibitors also caused cells to become shrunken and adopt a rounder shape. To further confirm this, we performed PI staining to assess the effects of both drug molecules. After staining and analysing the cells, we did not observe any changes in the cell cycle, suggesting that the structural changes may be due to other off-target effects that require further investigation. Despite cellular stress, the cell cycle data from treated cells were consistent with those from control cells (Figure 2A). Later, we performed membrane potential analysis to identify the cause of stress-induced apoptosis. Cells were treated as described and stained with JC1 dye. FACS data did not show a clear shift in the treatment cells. However, we detected another distinct population in the treated cells, which may indicate apoptosis and warrant further analysis (Figure 2B).

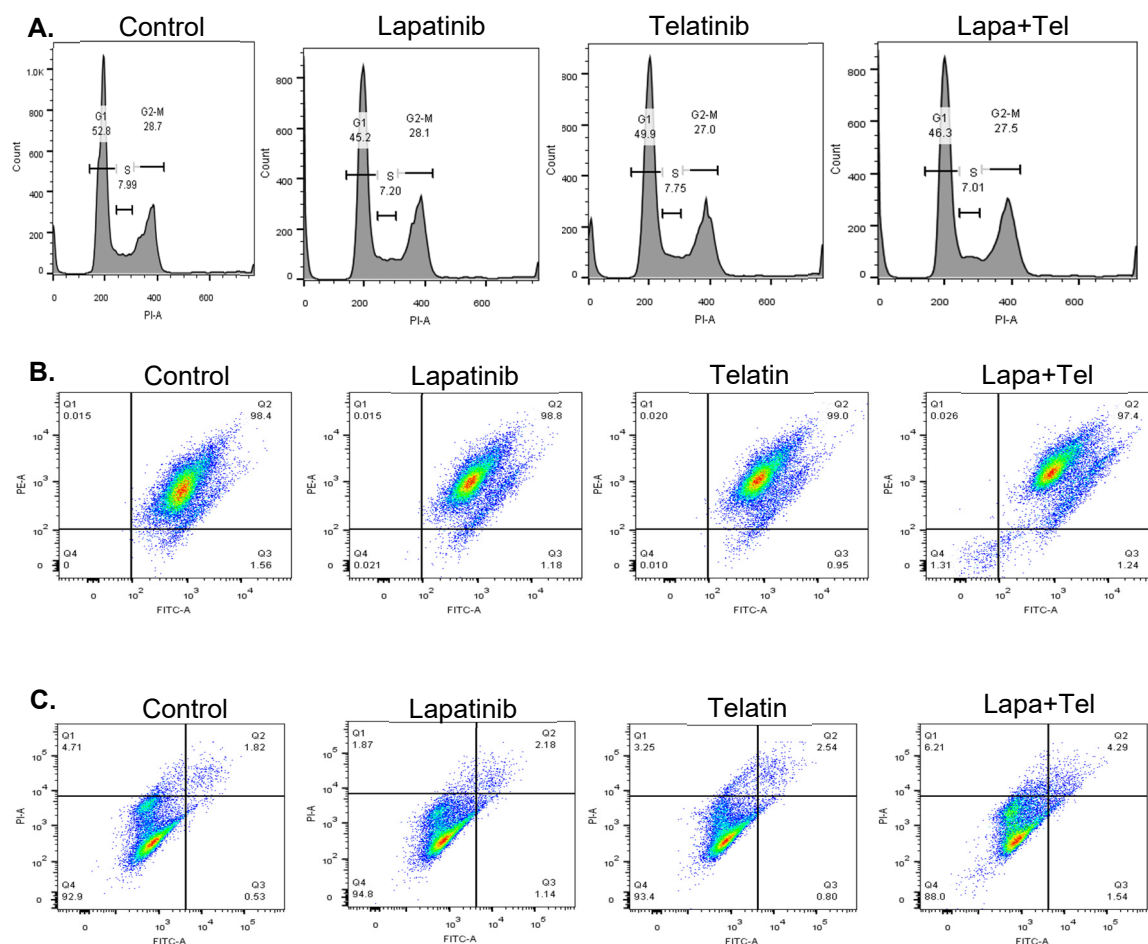


Figure 2. Cell cycle analysis of the MDA-MB-231 cell line after treatment with Lapatinib and Telatinib. (A) MDA-MB-231 cells were seeded in a 12-well plate and treated with Lapatinib, Telatinib, or both drugs. After 48 h, cells were harvested, and PI staining was performed for cell cycle analysis. Samples were analysed by flow cytometry. No significant effects were observed in treated cells compared to control cells. (B) Mitochondrial membrane potential was assessed in MDA-MB-231 cells following treatment with Lapatinib and Telatinib. Cells were seeded, treated with both drugs, and after 48 h, harvested, stained with JC-1, and analysed by FACS. No significant difference was detected between treated and control cells in the FACS analysis. (C) Apoptosis analysis in MDA-MB-231 cells after treatment with Lapatinib and Telatinib. The TNBC cells were analysed for cell death activity post-treatment. A combination of Lapatinib and Telatinib showed a slight increase in apoptotic cells. The percentage of double-positive apoptotic cells in the combination therapy was higher than in control cells.

3.3. A Combination of Lapatinib and Telatinib Initiates Early Apoptosis

TNBC cells lack the HER2 receptor, as well as ER and PR. Therefore, Lapatinib's effect should be minimal or negligible in this case. As explained earlier regarding the stressed morphology, this could result from the initiation of apoptosis. Cell cycle data and mitochondrial membrane potential measurements indicated that off-target effects under stress could lead to cell death. We performed an Annexin/PI assay to assess apoptosis after treatment with a combination of inhibitors. TNBC cells were treated with inhibitors, either alone or in combination, and then analysed for cell death. Our data showed a slight increase in double-positive cells with Lapatinib and Telatinib treatment compared to control cells. The number of double-positive cells increased in the combination treatment. This data suggests the initial potential of our inhibitory molecules, which could be further explored in other physiological assays to confirm their effects on cell behaviour within the tumour microenvironment (Figure 2C).

3.4. Lapatinib and Telatinib Inhibit Cellular Motility

TNBC cells have a high potential to metastasize to different regions of the body and colonise secondary sites. We observed early apoptosis induction in our previous data and performed invadopodia analysis. Our earlier results highlighted the importance of MMP2 and MMP9 degradation in cancer metastasis. To further confirm ECM degradation, we conducted invadopodia analysis. TNBC migrates through invadopodia formation facilitated by

the ECM in the tumour microenvironment. We treated the cells as described in the methods and imaged the gelatin-coated coverslips to assess TNBC motility. We found that the control group has a strong ability to degrade gelatin, as shown in Figure 3A. The control group showed numerous black patches, indicating a high risk of TNBC metastasis. Interestingly, we observed that the number of black patches indicative of gelatin degradation was reduced in the combination-treated group, with Lapatinib showing notable effectiveness (Figure 3A). Although the impact of Lapatinib was significant, the combination of Lapatinib and Telatinib also resulted in a marked reduction in gelatin degradation. Based on this data, we can infer that Lapatinib may have off-target effects in TNBC cells that influence their migratory properties within the tumour microenvironment.

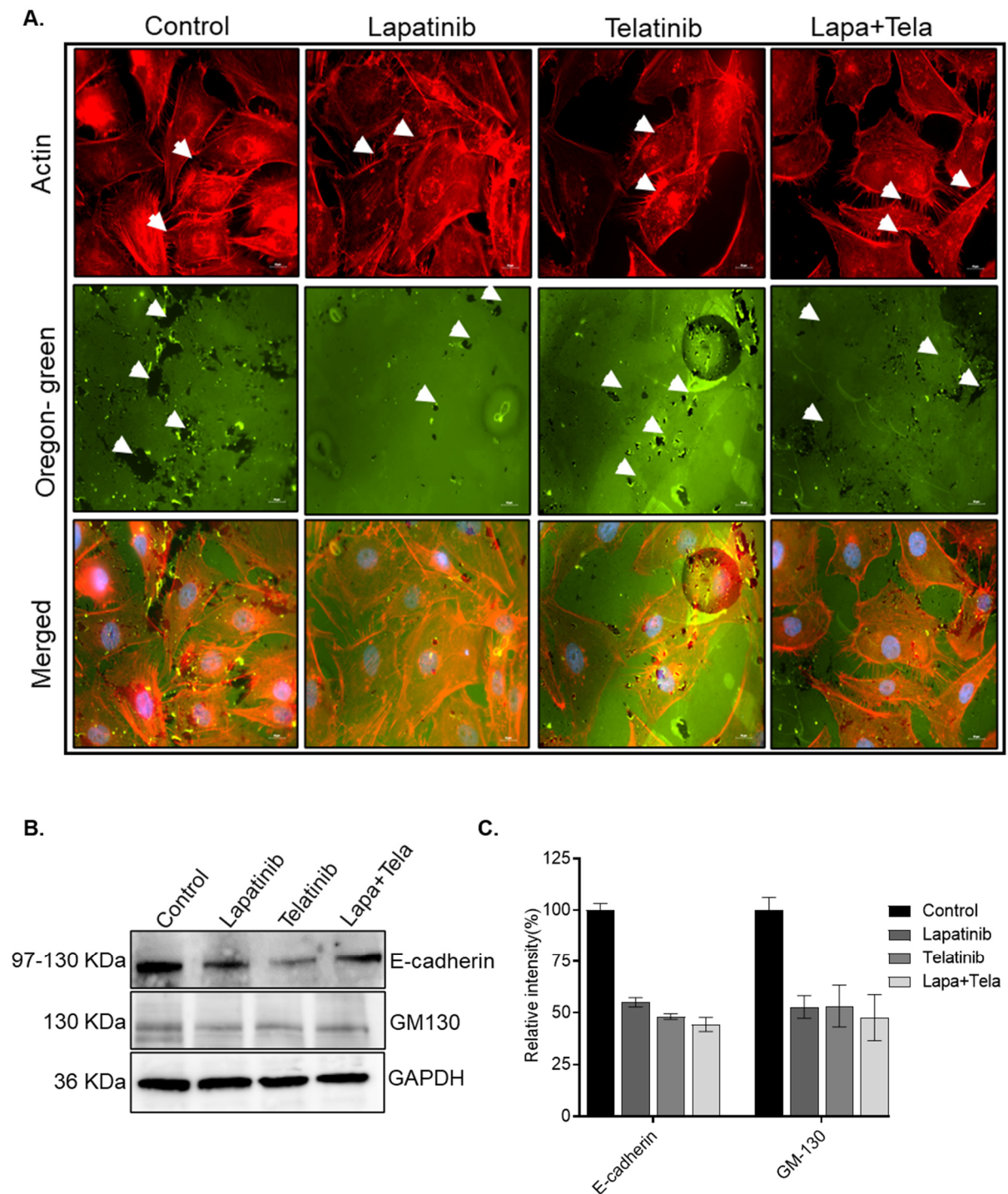


Figure 3. Extracellular gelatin degradation in MDA-MB231 breast cancer cells following treatment with Lapatinib and Telatinib. (A) Breast cancer cells were harvested and seeded onto a petri dish. After 48 h of treatment with both drugs, the cells were harvested again and seeded onto the top of precoated GFP coverslips in a 12-well plate. After 10–14 h, the cells were fixed with PFA, permeabilized with Triton X-100, stained with Actin-Phalloidin (Red), and mounted onto slides containing DAPI (for nuclear staining). The images were analysed with

a fluorescence microscope, and the data were generated. Numerous black patches were observed that are indicative of extensive extracellular matrix degradation and a high metastatic potential characteristic of TNBC. In contrast, the number of black patches representing gelatin degradation was markedly reduced in the combination-treated group as compared to the control groups. (B,C) Western blot analysis for E-cadherin and GM130 is shown here. Total cell lysates were prepared after treatment with the drugs, both alone and in combination. Western blot analysis was done to see the effect of these proteins: E-cadherin and GM130. The expression of these proteins was significantly decreased in the combination-treated group compared with the control. The graphs were generated using GraphPad Prism software v8.4, and the data were represented as mean \pm STD.

Cellular motility of cancer cells also depends on their interaction with nearby cells and the extracellular matrix (ECM). We examined E-cadherin expression and observed a significant change (Figure 3B,C). Cancer cells are characterised by their inability to adhere strongly to each other. This cell-cell adhesion is usually mediated by membrane proteins such as cadherins and occludins. Among these, E-cadherin is a well-known tumour suppressor protein that serves as a prognostic marker for breast cancer. The frequent downregulation of E-cadherin is observed in aggressive tumours and is associated with the progression, invasion, and metastasis of these tumours [37,38]. There is substantial evidence indicating that E-cadherin expression decreases in high-grade, aggressive, estrogen receptor-negative, and metastatic breast cancers. In breast tumours, reduced E-cadherin expression has been noted in 50% of invasive ductal carcinomas and 90% of invasive lobular carcinomas. Introducing E-cadherin into these cell lines impeded their ability to invade *in vitro* [39].

3.5. A Combination of Lapatinib and Telatinib Modulates a Metastatic Marker

The fundamental infrastructure for cell movement is provided by the cytoskeleton, which consists of microtubules, intermediate filaments, and actin filaments. Among these, the actin cytoskeleton regulates cell motility in breast cancer cells. Numerous proteins can bind to or bundle actin, including MENA [40,41]. MENA promotes actin polymerisation by disrupting inhibitory capping proteins, thereby supporting continued polymerisation and enhancing cell motility in response to growth factors [42]. In breast cancer, MENA plays a crucial role in the tumour microenvironment related to metastasis, with its density positively associated with the risk of distal metastasis [27]. Furthermore, MENA inhibition in breast cancer mouse models reduces mortality and limits metastatic potential. In human patients, changes in isoforms MENA11a and MENA^{INV} are associated with patient outcomes. While MENA11a expression is low in invasive breast cancer subtypes, high levels of MENA^{INV} correlate with increased metastasis and poorer prognosis [43]. Given their role in cancer metastasis, we monitored the protein's expression after treatment with the novel drug combination. Fluorescent-stained MENA, β -actin, α -tubulin, and Occludin were found to be downregulated following treatment with Lapatinib and Telatinib (Figure 4A,B). Since these molecules are linked to increased aggressiveness in cancer cells, their downregulation after treatment may indicate improved disease outcomes and prognosis.

Outside MENA, we also observed the effect of these drugs on Occludin and TGF- β 1. Occludin is an essential membrane protein found at tight junctions (TJs). It has become clear that TJs are crucial structures that cancer cells must bypass to metastasize successfully. Although occludin was among the first TJ proteins identified, its specific role within the TJ remains poorly understood [44]. Transforming growth factor-beta 1 (TGF- β 1) was initially identified for its role in mammary epithelial development. Dysregulation of TGF- β in a tumour contributes to the progression toward malignancy. The expression of active TGF- β 1 is significantly higher in the plasma of patients with breast cancer. Additionally, there is a loss of expression of downstream signaling components in solid carcinomas. TNBCs treated with anti-TGF- β agents are less likely to metastasize to the lungs and bones [45]. The presence of a TGF- β 1 pro allele has been reported to increase TGF- β 1 secretion *in vivo* and is linked to a higher risk of breast cancer. Evidence also suggests that SNPs in TGF- β 1 and TGF- β R1 may contribute to the development of breast cancer. A meta-analysis on this topic confirmed these findings and showed that the TGF- β 1 is associated with an increased risk of developing breast cancer [46,47]. Cells treated with the drug combination *in vitro* showed a decrease in pro-metastatic Occludin and TGF- β 1 (Figure 4C). The quantification of the Western blot experiment is seen in Figure 4D. The combination treatment showed a decreased expression of these molecules as compared with the control. Given the role that elevated TGF- β 1 plays in breast cancer progression, the decrease in its expression could suggest a better prognosis.

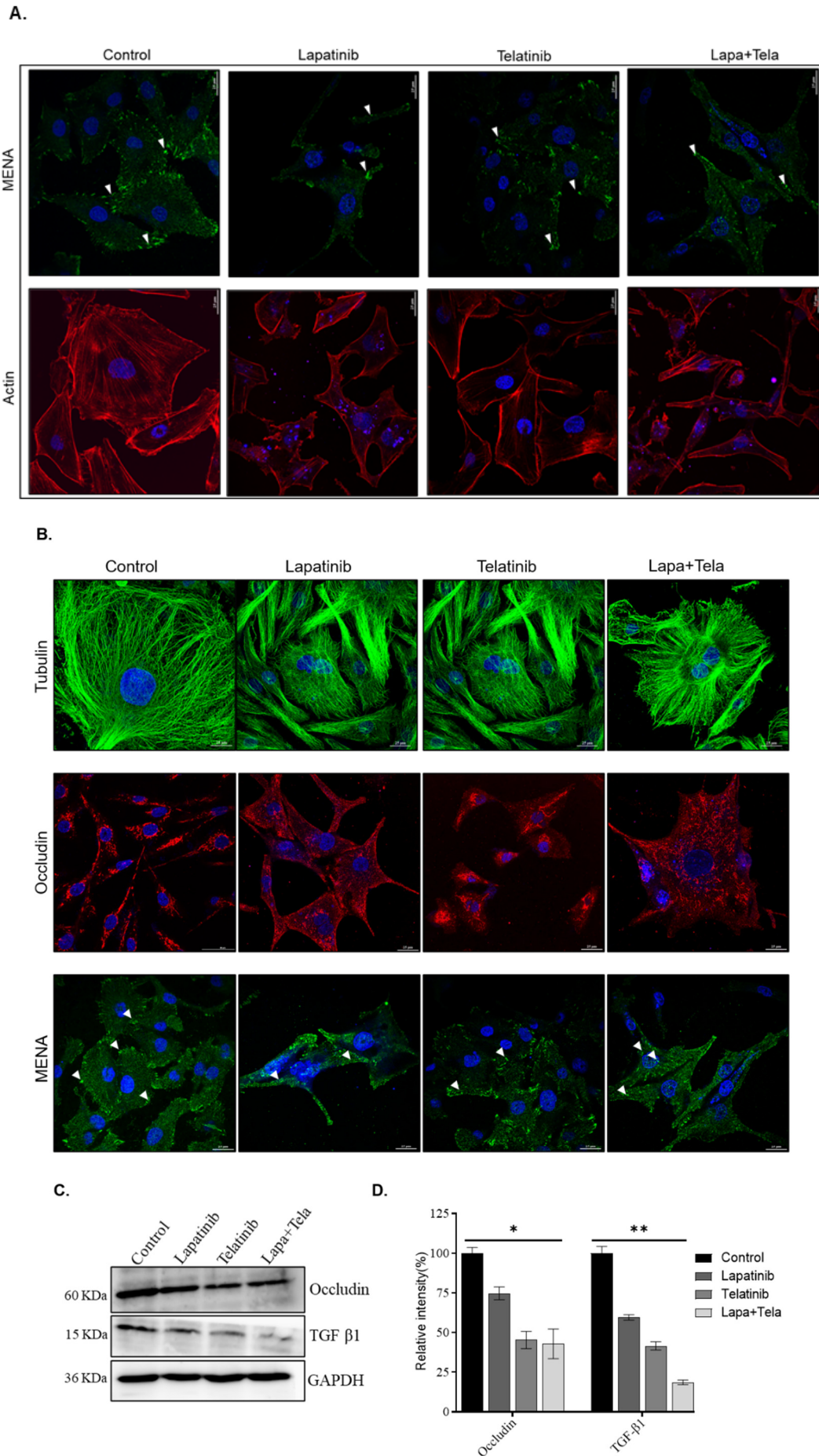
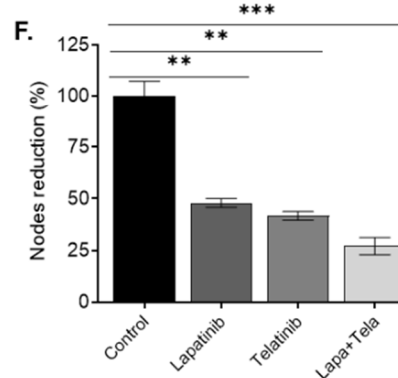
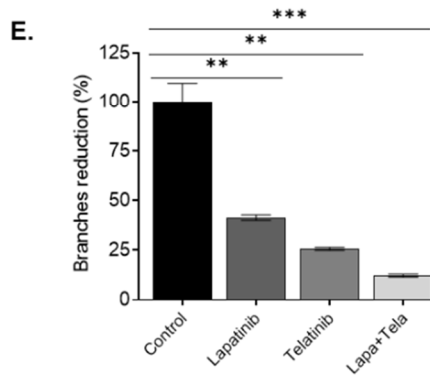
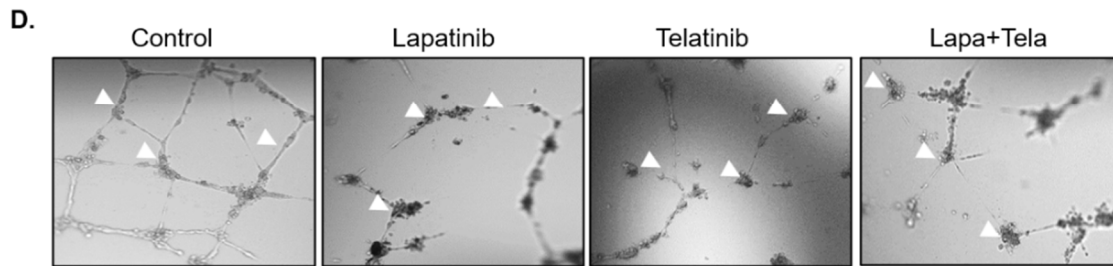
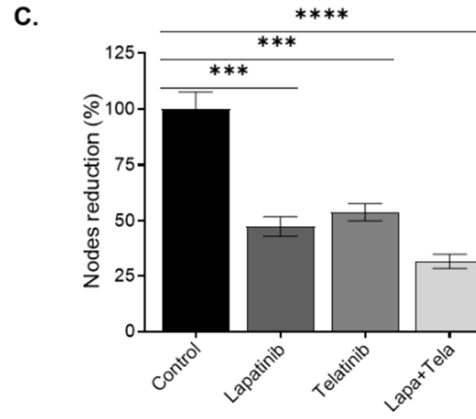
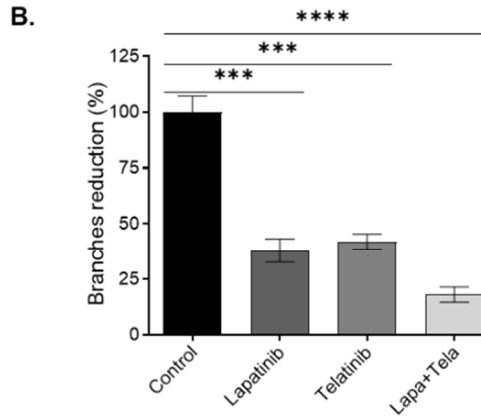
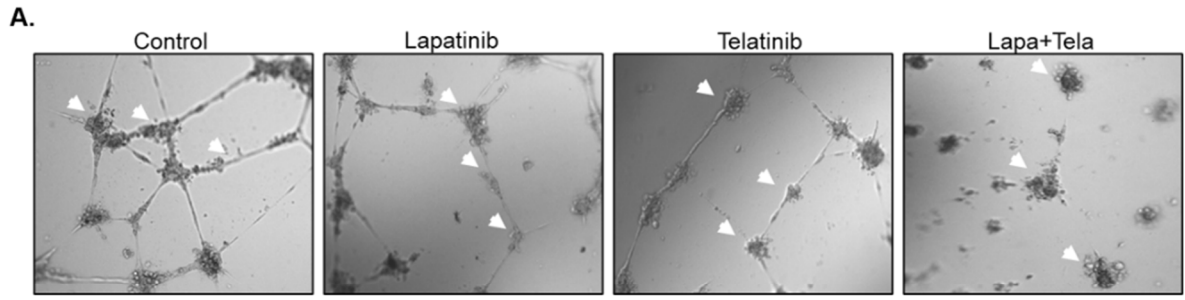


Figure 4. The combination of Lapatinib and Telatinib treatment showed decreased metastatic markers. (A,B) MDA-MB-231 and MDA-MB-453 cells were treated with the drugs alone or in combination, and after 24 h,

slides were prepared and stained with metastatic, Tight junction, and cytoskeletal markers such as MENA, β -actin, α -tubulin, and Occludin. The slides were analysed using a Confocal microscope. The expression of these molecules/markers was greatly reduced in the combination-treated group compared to the control group. (C) Breast cancer cells were grown in petri plates and treated with this drug combination regimen. Cell lysates were prepared in RIPA buffer containing protease inhibitors and analysed by Western blotting for the following metastatic markers. Expression of Occludin and TGF- β 1 was significantly reduced in the combination-treated group compared to the control group. (D) The graphs were generated using GraphPad Prism software v8.4, and the data were represented as mean \pm STD. The significance levels were calculated as * $p < 0.05$ and ** $p < 0.01$.

3.6. A combination of Inhibitors Effectively Reduced Tumour-Induced Angiogenesis

Tumour-induced angiogenesis is the primary source of tumour development in hypoxic conditions. These angiogenic tubes help tumours circulate and colonise secondary sites in the body, enabling effective growth. We wanted to explore the effects of the treatments Lapatinib and Telatinib on TNBC and non-TNBC-induced angiogenesis in tumour microenvironment conditions. To do this, we treated TNBCs and MDA-MB-453 with drug molecules and collected and quantified TCM as discussed in the method section. Primary HUVEC cells were grown and incubated with TCM at equal concentrations. We found that treatment with Lapatinib and Telatinib strongly inhibits the tube-forming capacity of HUVECs on ECM. We quantified the nodes and tube-formation data and observed a significant reduction relative to control cells (Figure 5A–F). To analyse the molecular behaviour of molecules involved in tumour-induced angiogenesis, we conducted Western blot analysis. Platelet Endothelial Cell Adhesion Molecule 1 (PECAM-1) is expressed in several cancers. It has been found to inhibit apoptosis, promote cancer progression, and confer therapeutic resistance [48]. It was found to decrease proliferation and increase cancer cell motility and morphology [49]. There is also evidence for its role in angiogenesis, as shown by reduced vasculature when PECAM-1 was inhibited (Figure 5G). Vascular Endothelial Growth Factor Receptor 2 (VEGFR-2) is a membrane-bound tyrosine kinase receptor that plays a crucial role in tumour angiogenesis [50]. It is known that tumours secrete VEGF to promote blood vessel formation, which can lead to tumour metastasis. In breast cancer, VEGFR-2 mRNA was found to be upregulated and was associated with decreased survival in patients [51]. Recent studies show that VEGF maintains cancer stem cells by activating the JAK2/STAT3 pathway in breast cancer [52]. Its role in regulating angiogenesis, metastasis, and stem cell renewal has made VEGFR-2 an important therapeutic target. We also analysed the expression of epidermal growth factor receptor (EGFR), a receptor tyrosine kinase in the ErbB family. Gene expression studies have shown that EGFR is overexpressed in 50–70% of basal-like breast tumours and in 18–35% of all breast cancers [53]. These EGFRs are crucial in supporting cancer cell survival and proliferation. This occurs through a significant increase in receptor levels at the protein level. Additionally, tumours can also express dysregulated EGFR1 signalling via EGFR mutations, elevated ligand expression, or heterodimerisation with other EGFRs [54]. While these mutations and gene amplification are rare in breast cancers, EGFR can be elevated through polysomy, which increases copy number. This leads to increased metastasis and poorer prognosis [55]. The resulting constitutive activation of downstream signaling pathways, including the PI3K/AKT and MAPK/ERK cascades, promotes uncontrolled cell growth, resistance to apoptosis, and enhanced metastatic potential, making EGFR an attractive therapeutic target in breast cancer, particularly in basal-like and triple-negative subtypes where conventional hormone-targeted therapies are ineffective. Our combination approach depicted a significant effect on these molecules. PECAM-1, VEGFR-2, and EGFR were downregulated by the combination approach, supporting inhibition of tumour-induced angiogenesis (Figure 5G,H).



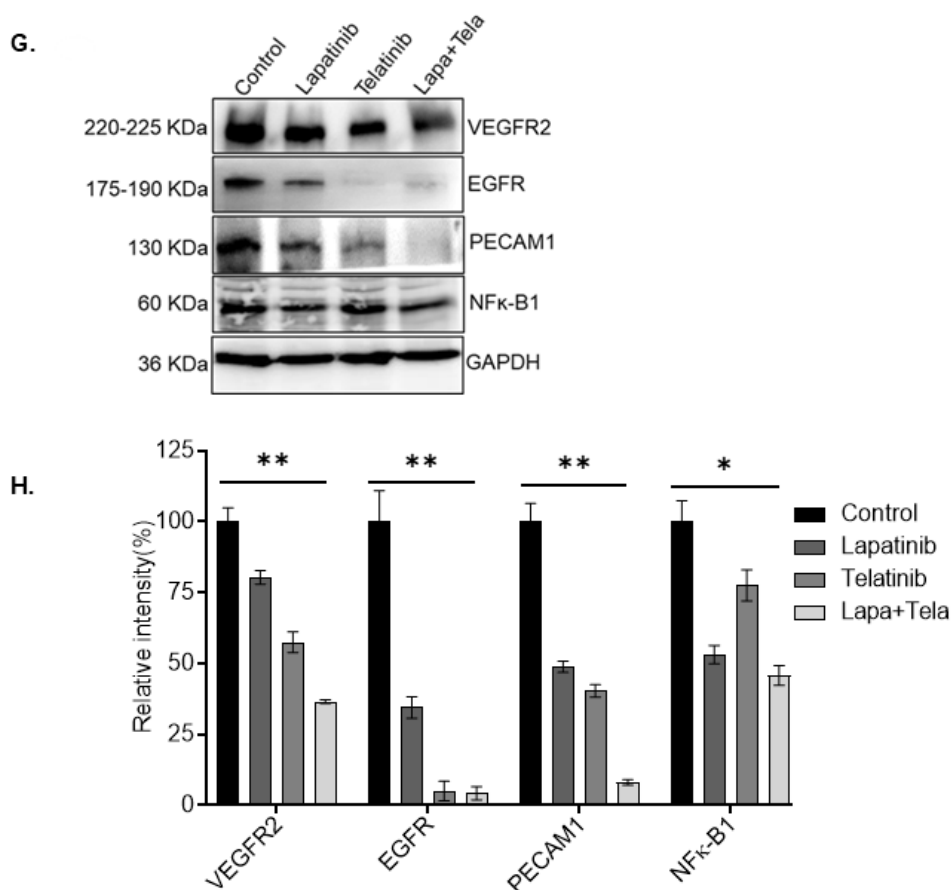


Figure 5. Treatment with a combination of drugs reduces the angiogenic potential of primary HUVEC cells.

(A,D) First, TNBC cells treated with Lapatinib and Telatinib alone or the combinations and TCM were collected after 24 and 48 h. The TCMs were then concentrated and taken in equal concentrations for all the groups. Next, Primary cells, HUVECs, were plated onto a 96-well plate coated with Matrigel in the presence of equal TCM concentrate from the control and treated groups. Tubes and branches were observed after 4, 8, and 12 h. (B,C,E,F) The relative graphs showed that the tubes and nodes formation were significantly reduced in the combination-treated group as compared to the control group. Tubes and nodes formation were quantified using AngioTool software v0.6a and the data were represented as mean \pm STD. (G,H) The total cell lysates were collected from the treated and control groups, and the western blot experiment was analysed for the following proteins: VEGFR-2, PECAM1, EGFR, and NF- κ B1. The expression of all these proteins showed a significant decrease in the combination-treated group compared with the control group. The graphs were generated using GraphPad Prism software v8.4, and the data were represented as mean \pm STD. The significance levels were calculated as * $p < 0.05$, ** $p < 0.01$, *** $p < 0.001$, **** $p < 0.0001$.

3.7. Lapatinib and Telatinib treatment induces stress in breast cancer cells

Our data indicated that targeting cancer cells with a combination of our molecules causes morphological changes. This may result from a shift in cell state from healthy to stressed, reducing the metastatic potential of cancer cells. To explore this further, we performed a stress response analysis on the treated cells. We used a proteome array to analyse the treated cells. Tissue culture media from the treated cells, collected as described in the methods section, were used in equal amounts for the experiment. Results showed significant upregulation and downregulation of key stress-related molecules. HSP70 and HSP60 are primary stress markers. Their expression increased significantly when Lapatinib and Telatinib were combined with SOD2. The levels of heat shock proteins provide insights into stress-induced morphological changes in cells (Figure 6A,B).

We further elaborated on the molecules that are the key regulators of cancer and are associated with stress-induced responses. ADAMTS1 (A Disintegrin and Metalloproteinase with Thrombospondin Motifs 1) is a zinc-binding metalloprotease that is found in several tissues and plays a role in tissue remodelling during cancer progression [56]. Studies have shown that cancer-associated fibroblasts (CAFs) secrete ADAMTS1, which in turn promotes cancer cell invasion. Interestingly, CAF secreted ADAMTS1 was found to be the highest in breast cancer cell lines [57]. In breast cancer, the upregulation of ADAMTS1 is linked to metastasis, as witnessed in *in vivo*

models. In these models, loss of ADAMTS1 significantly impeded tumour progression and metastasis [58]. The human Carcinoembryonic Antigen-related Cell Adhesion Molecule 1 (CEACAM1) plays a central role in maintaining normal tissue structure and polarity [59]. Evidence links CEACAM1 to cell-cycle inhibitory proteins, suggesting a connection between tissue architecture and cell-cycle regulation [60]. CEACAM1 is known to play a role in lumen formation during morphogenesis and could revert breast cancer cells to normal [61]. Therefore, the loss of this link could impede the regulation of the cell cycle and tumorigenesis. Data from studies also show a systematic down-regulation of CEACAM1 mRNA and protein in breast cancer cell lines, leading to aggressive proliferation [62]. To identify important biomarkers dysregulated in breast cancer, a cell stress proteome array was performed. The results of this assay led us to monitor the expression of pro-metastatic markers ADAMTS1, CEACAM1, and HIF1 α . Our immunoblot results showed a profound decrease in metastatic and vascular mimicry marker levels after treatment with the drug combination (Figure 6C,D). The Schematic representation shows that these two drug combinations synergistically inhibit breast cancer cell invasion and angiogenesis across multiple pathways (Figure 7).

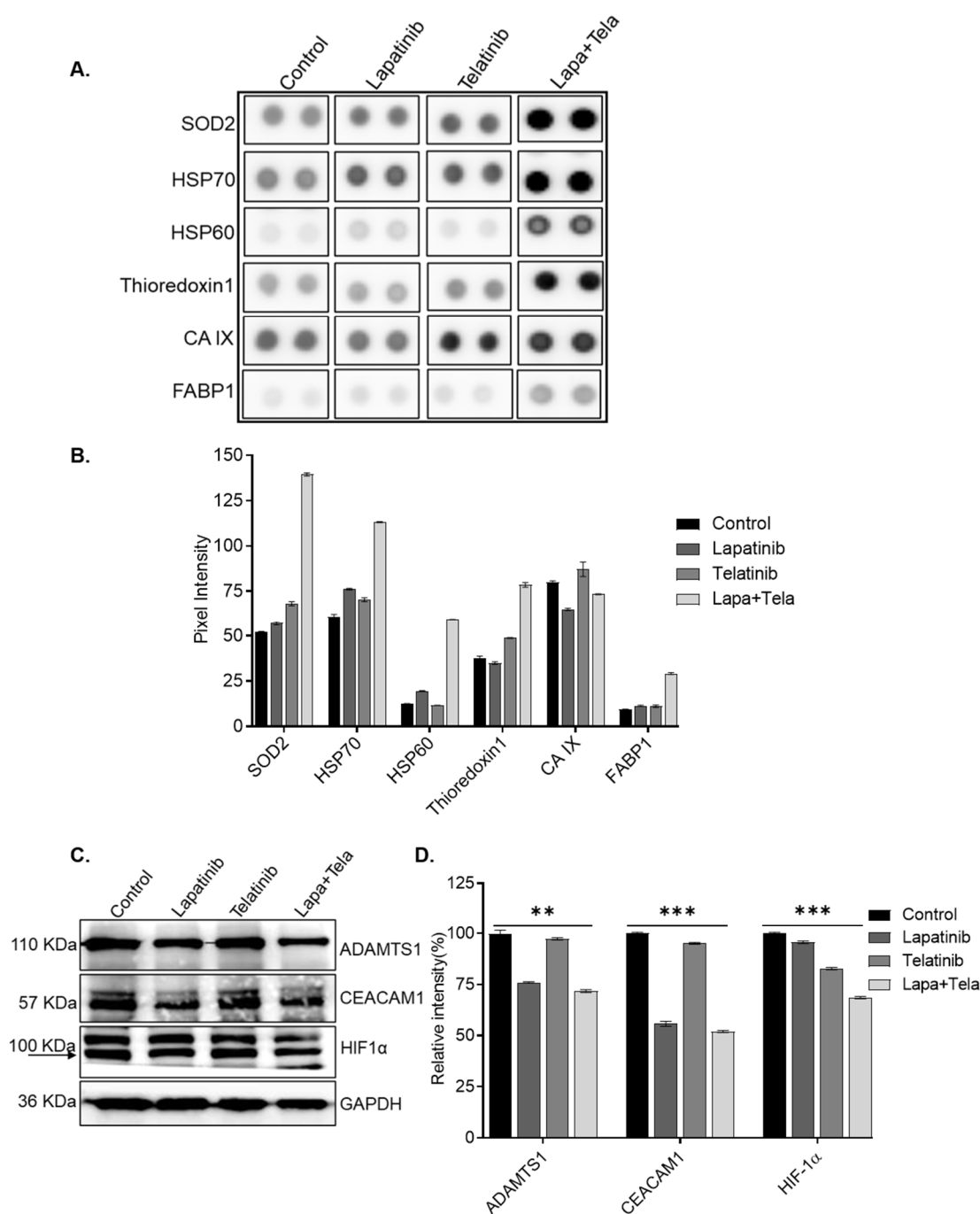


Figure 6. The Cell Stress Array analysis showed upregulation of stress markers in the combination treatment. (A) MDA-MB-231 cells were seeded and grown in a Petri dish. After reaching the confluency of about

65–80%, cells were treated with all the combinations of the drug molecules. After 24, 48 and 72 h, cell lysates were prepared, and protein concentration was measured using the Bradford method. Following the manufacturer’s protocol, the cell stress array experiment was performed, and stress markers-including SOD, HSP-60, HSP-70, CA XI, and FABP1-were identified. (B) The dots were quantified using ImageJ, and graphs were made with pixel intensity as the comparison metric. As compared to the control group, these stress markers were significantly increased in the combination-treated group. (C) Next, we identified a few stress-induced markers and analysed them using a Western blotting experiment. Cells were seeded, treated, and prepared for total cell lysates with RIPA buffer and protease inhibitor. The expression of all these proteins was significantly reduced in the combination treatment group as compared to the control group. (D) The graphs were generated using GraphPad Prism software v8.4, and the data were represented as mean ± STD. The significance levels were calculated as ** $p < 0.01$, and *** $p < 0.001$.

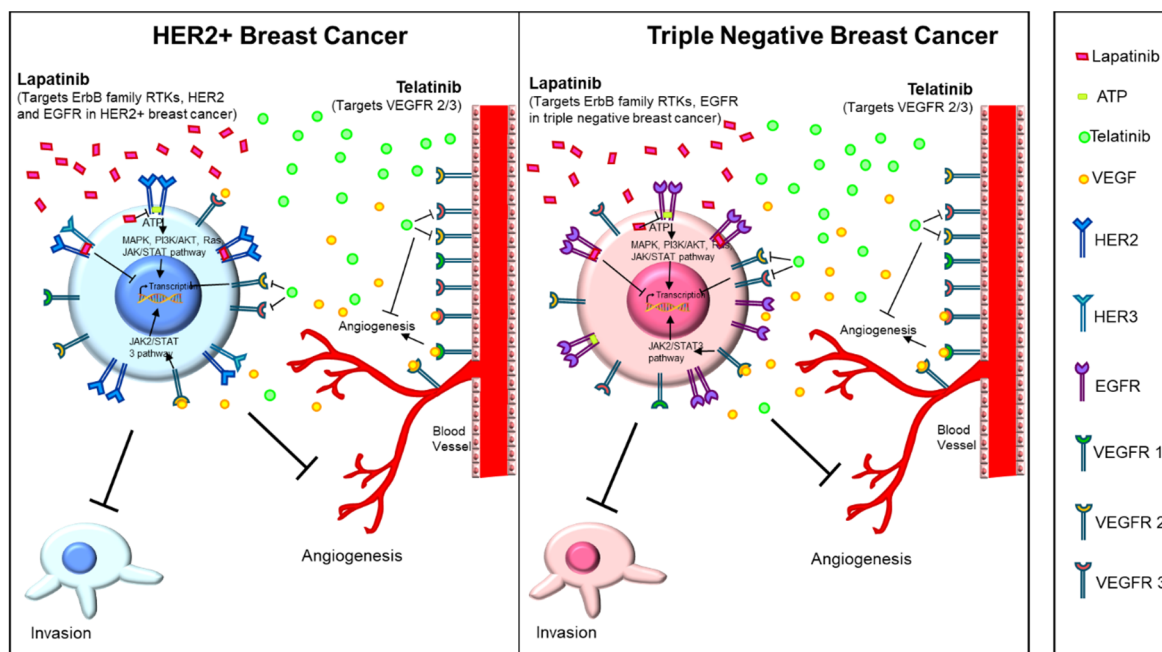


Figure 7. A schematic representation showing the effects of Lapatinib and Telatinib, which are inhibitory molecules, in HER2+ and TNBC cells.

4. Discussion

Breast tumours are molecularly classified to enable efficient treatment with targeted therapies. The three major subtypes are luminal, HER2+, and basal-like tumours. The luminal tumours have shown a high expression of estrogen receptor and progesterone receptor, and the therapy is provided in the form of anti- hormonal therapies. The HER2+ subtype has ERBB2 overexpression and is targeted with anti-HER2 therapies. Basal-like tumours are characterised by the absence of receptors such as ER, PR, or HER2. They are called TNBCs [63]. Among all new breast cancer patients, two-thirds of patients are ER-positive. Estrogen and Estrogen receptors play an essential role in the progression of breast cancer. Majorly, hormonal therapy is provided to breast cancer patients expressing ER. The Food and Drug Administration (FDA) has approved three selective estrogen receptor modulators (SERMs), namely Toremifene, Raloxifene, and Tamoxifen, that competitively bind with the ER [64]. However, the major obstacle is the triple-negative breast cancer subtype (ER⁻, PR⁻, and HER2⁻), which poses a major therapeutic challenge [65]. TNBC cases have poor survival due to a deficiency of effectively targeted agents that could efficiently induce effective treatments in other breast cancer subtypes. [66,67]. Prior studies have shown that VEGFR-2 inhibition can directly suppress breast cancer cell proliferation and induce apoptosis through mitochondrial ROS production and downregulation of the Akt–PGC1 α –TFAM axis, indicating that VEGFR-2 signaling contributes not only to angiogenesis but also to tumour-cell survival and metabolism in certain contexts [68]. In this context, our dual HER2/VEGFR-2-targeting strategy differs mechanistically from VEGFR-2-only inhibition by simultaneously blocking HER2-driven oncogenic signaling and VEGFR-2-mediated angiogenic signaling, thereby addressing both intrinsic tumour-cell growth and microenvironmental vascular support. Our findings suggest that concurrent inhibition of these two pathways may produce a more comprehensive antitumour effect, potentially through additive or synergistic suppression of proliferation and pro-survival signaling, although

formal synergy will require further dedicated study. Compared with previously reported receptor-targeting approaches such as bispecific antibodies or combination therapies, our strategy is distinctive in its specific emphasis on HER2 and VEGFR-2 as complementary therapeutic targets within a single framework. Overall, these results support the translational potential of dual HER2/VEGFR-2 inhibition as a strategy that may impair tumour proliferation, angiogenesis, and possibly metabolic adaptations that contribute to tumour progression.

Precision Medicine can be seen as the collection of an individual's cancer genomic data and tailoring appropriate treatment to that patient based on that data. The main reason for using precision medicine in cancer therapeutics is that cancer is a genomic disease characterised by mutations in oncogenes and tumour suppressor genes that drive cancer progression through various signaling and molecular pathways. TNBC is highly metastatic in nature and commonly leads to the death of patients. The most common metastatic site for breast cancer is the Bone. Similarly, whilst anti-HER2 therapies, such as trastuzumab in combination with chemotherapy, have significantly increased overall survival for patients with early and advanced HER2-amplified breast cancer, resistance mechanisms lead to recurrent and metastatic disease [69,70]. There are no targeted therapies for TNBC currently and they account for about 10–20% of all breast cancers. TNBC tumours have a high rate of recurrence and an aggressive phenotype.

The survival rate for women with TNBC is less than 30%. TNBC is not limited to the basal-like phenotype and correlates with other subtypes, including luminal A (17%), normal breast-like (12%), luminal B (6%), HER2 (6%), and unclassified (12%). Thus, it has varying sensitivity to various targeted therapies [71,72]. Treatment relies on surgery, chemotherapy and radiotherapy; however, the disease-free interval with neoadjuvant or adjuvant therapy is shorter and metastatic disease is more aggressive than other types of breast cancer [73,74]. Precision medicine, in contrast, can also be applied to healthy individuals to identify the risk of developing certain types of cancer through genetic evaluation of predisposition genes and to provide treatment accordingly. But analysing the genome presents many challenges, as we must first identify somatic and germline mutations and distinguish actionable driver mutations from the larger set of passenger mutations. Earlier reports demonstrated that TNBC patients treated with systemic chemotherapies could produce chemoresistance, which consequently causes relapse with a worse prognosis [75,76]. The FDA approved lapatinib for metastatic breast cancer treatments with other chemotherapeutic agents for EGFR and/or HER2-expressing head and neck carcinoma and salivary gland carcinoma [77]. Also, lapatinib was effective when combined with chemoradiotherapy for locally progressive head and neck squamous cell carcinoma (HNSCC) [78]. Many reports demonstrate that TKIs, including gefitinib and lapatinib, induce responses in TNBC cells [79–88].

We utilized a novel combination of two inhibitory molecules, i.e., Lapatinib and Telatinib, in our studies. The effect of Lapatinib is strong in HER2+ cells; we observed a significant reduction in TNBC cell proliferation. Although lapatinib is primarily a dual EGFR/HER2 inhibitor, its effects in HER2-negative cells may also reflect inhibition of EGFR signaling and, potentially, additional off-target kinases. Initially, we found that Lapatinib and Telatinib effectively reduced cell survival at 5 μ M. Cellular shape was distorted after treatment with these molecules; cells shrank after lapatinib treatment and became round with Telatinib. A combination of these molecules strongly reduced cell survival and instigated morphological changes instantly. This was further confirmed with various experiments. To obtain further insight into the effects of these molecules on TNBC cells, we performed cell cycle analysis and mitochondrial membrane potential assays to evaluate mechanisms of cell death. However, cells were getting stressed after the treatment with these molecules; the effect on cell cycle progression was not significant. Later, we performed an Annexin/PI labelling assay because the membrane potential analysis did not confirm the stress conditions.

We found a slight increase in double-positive cells in Annexin/PI labelling, indicating that Lapatinib and Telatinib are gradually inducing stress in TNBC cells and increasing the number of early apoptotic cells. These induced early apoptotic cells may lose physiological properties, such as cell adhesion and migration. We later investigated cellular invasion properties using a gelatin degradation assay or an invadopodia assay and found a significant reduction.

Neovascularization and angiogenesis are key features of metastasis and cancer-related mortality. Finally, we analysed the tumour microenvironment using the angiogenic capacity of primary HUVECs. One of the most successful models developed in the case of precision medicine is the anti-HER2 therapies, as HER2 was considered to have the worst prognosis, as it is highly malignant, but now, due to the advent of HER2 receptor targeted therapies, it has a good prognosis. Tissue culture media from TNBC cells, treated with lapatinib alone and in combination with telatinib, show a strong reduction in the angiogenic potential of primary HUVECs. Later, we showed a schematic representation of our hypothesis, which suggests the effect of Lapatinib on TNBC cells. Our study provides input on the use of novel drug combinations for further studies aimed at inhibiting cancer progression in TNBC cells.

Author Contributions: M.R. and N.K. designed the study. M.R., N.K. and S.S. wrote the manuscript. M.R. and N.K. performed the experiments. All authors have read and agreed to the published version of the manuscript.

Funding: The Shiv Nadar Foundation is providing a PhD fellowship to Masoom Raza. This research received no external funding.

Institutional Review Board Statement: Not applicable.

Informed Consent Statement: Not applicable.

Data Availability Statement: Not applicable.

Acknowledgements: The Shiv Nadar Foundation was recognized for providing a PhD fellowship to Masoom Raza. Naveen Kumar was working as a Research Associate.

Conflicts of Interest: The authors declare no conflict of interest.

Use of AI and AI-Assisted Technologies: No AI tools were utilized for this paper.

Abbreviations

TNBC: Triple Negative Breast Cancer, HUVEC: Human Umbilical Vein Endothelial Cell, HER-2: Human Epidermal Growth Factor Receptor-2, ER/PR: Estrogen/Progesterone, MDA-MB-231: MD Anderson-Metastatic Breast-231, MMP2 and 9: Matrix Metalloproteinase2 and 9, EGFR: Epidermal Growth Factor Receptor

References

1. Ferlay, J.; Soerjomataram, I.; Dikshit, R.; et al. Cancer incidence and mortality worldwide: Sources, methods and major patterns in GLOBOCAN 2012. *Int. J. Cancer* **2015**, *136*, E359–386.
2. Raza, M.; Kumar, N.; Nair, U.; et al. Current updates on precision therapy for breast cancer associated brain metastasis: Emphasis on combination therapy. *Mol. Cell. Biochem.* **2021**, *476*, 3271–3284.
3. Bray, F.; Ferlay, J.; Soerjomataram, I.; et al. Global cancer statistics 2018: GLOBOCAN estimates of incidence and mortality worldwide for 36 cancers in 185 countries. *CA Cancer J. Clin.* **2018**, *68*, 394–424. <https://doi.org/10.3322/caac.21492>.
4. American Cancer Society. *Breast Cancer Facts and Figures 2024–2025*; American Cancer Society: Atlanta, GA, USA, 2024; 28p.
5. Kuchenbaecker, K.B.; Hopper, J.L.; Barnes, D.R.; et al. Risks of Breast, Ovarian, and Contralateral Breast Cancer for BRCA1 and BRCA2 Mutation Carriers. *Jama* **2017**, *317*, 2402–2416. <https://doi.org/10.1001/jama.2017.7112>.
6. Chen, S.; Parmigiani, G. Meta-analysis of BRCA1 and BRCA2 penetrance. *J. Clin. Oncol. Off. J. Am. Soc. Clin. Oncol.* **2007**, *25*, 1329–1333. <https://doi.org/10.1200/jco.2006.09.1066>.
7. Ford, D.; Easton, D.F.; Bishop, D.T.; et al. Risks of cancer in BRCA1-mutation carriers. *Lancet* **1994**, *343*, 692–695.
8. Antoniou, A.; Pharoah, P.D.; Narod, S.; et al. Average risks of breast and ovarian cancer associated with BRCA1 or BRCA2 mutations detected in case series unselected for family history: A combined analysis of 22 studies. *Am. J. Hum. Genet.* **2003**, *72*, 1117–1130.
9. Weigelt, B.; Geyer, F.C.; Reis-Filho, J.S. Histological types of breast cancer: How special are they? *Mol. Oncol.* **2010**, *4*, 192–208. <https://doi.org/10.1016/j.molonc.2010.04.004>.
10. Diana Schlamadinger, P. Molecular Subtypes of Breast Cancer: Types, Diagnosis, & Treatment Guide. Available online: <https://www.bcrf.org/about-breast-cancer/molecular-subtypes-breast-cancer/> (accessed on 1 June 2026).
11. McDonald, E.S.; Clark, A.S.; Tchou, J.; et al. Clinical Diagnosis and Management of Breast Cancer. *J. Nucl. Med. Off. Publ. Soc. Nucl. Med.* **2016**, *57*, 9s–16s. <https://doi.org/10.2967/jnumed.115.157834>.
12. Takada, M.; Toi, M. Cryosurgery for primary breast cancers, its biological impact, and clinical outcomes. *Int. J. Clin. Oncol.* **2019**, *24*, 608–613. <https://doi.org/10.1007/s10147-019-01448-4>.
13. Nagini, S. Breast Cancer: Current Molecular Therapeutic Targets and New Players. *Anti-Cancer Agents Med. Chem.* **2017**, *17*, 152–163, doi:doi:10.2174/1871520616666160502122724.
14. Konig, I.R.; Fuchs, O. What is precision medicine? *Eur. Respir. J.* **2017**, *50*, 1700391. <https://doi.org/10.1183/13993003.00391-2017>.
15. Jia, H.; Truica, C.I.; Wang, B.; et al. Immunotherapy for triple-negative breast cancer: Existing challenges and exciting prospects. *Drug Resist. Updates* **2017**, *32*, 1–15. <https://doi.org/10.1016/j.drug.2017.07.002>.
16. Bayat Mokhtari, R.; Homayouni, T.S.; Baluch, N.; et al. Combination therapy in combating cancer. *Oncotarget* **2017**, *8*, 38022–38043. <https://doi.org/10.18632/oncotarget.16723>.
17. Mishra, V.S.; Kumar, N.; Raza, M.; et al. Amalgamation of PI3K and EZH2 blockade synergistically regulates invasion and angiogenesis: Combination therapy for glioblastoma multiforme. *Oncotarget* **2020**, *11*, 4754–4769. <https://doi.org/10.18632/oncotarget.27842>.

18. Braga, S. Resistance to Targeted Therapies in Breast Cancer. In *Cancer Drug Resistance*; Humana Press: New York, NY, USA, 2016; Volume 1395, pp. 105–136. https://doi.org/10.1007/978-1-4939-3347-1_8.
19. Wang, T.; Narayanaswamy, R.; Ren, H.; et al. Combination therapy targeting both cancer stem-like cells and bulk tumor cells for improved efficacy of breast cancer treatment. *Cancer Biol. Ther.* **2016**, *17*, 698–707. <https://doi.org/10.1080/15384047.2016.1190488>.
20. Mboge, M.Y.; Mahon, B.P.; McKenna, R.; et al. Carbonic anhydrases: Role in pH control and cancer. *Metabolites* **2018**, *8*, 19.
21. Shen, Y.; Vignali, P.; Wang, R. Rapid Profiling Cell Cycle by Flow Cytometry Using Concurrent Staining of DNA and Mitotic Markers. *Bio-Protocol* **2017**, *7*, e2517. <https://doi.org/10.21769/BioProtoc.2517>.
22. Sivandzade, F.; Bhalerao, A.; Cucullo, L. Analysis of the Mitochondrial Membrane Potential Using the Cationic JC-1 Dye as a Sensitive Fluorescent Probe. *Bio-Protocol* **2019**, *9*, e3128. <https://doi.org/10.21769/BioProtoc.3128>.
23. Kumar, N.; Raza, M.; Sehrawat, S. Intuitive repositioning of an anti-depressant drug in combination with tivozanib: Precision medicine for breast cancer therapy. *Mol. Cell. Biochem.* **2021**, *476*, 4177–4189.
24. Rieger, A.M.; Nelson, K.L.; Konowalchuk, J.D.; et al. Modified annexin V/propidium iodide apoptosis assay for accurate assessment of cell death. *J. Vis. Exp.* **2011**. <https://doi.org/10.3791/2597>.
25. Smith, E.; Palethorpe, H.M.; Tomita, Y.; et al. The Purified Extract from the Medicinal Plant *Bacopa monnieri*, Bacopaside II, Inhibits Growth of Colon Cancer Cells *In Vitro* by Inducing Cell Cycle Arrest and Apoptosis. *Cells* **2018**, *7*, 81. <https://doi.org/10.3390/cells7070081>.
26. Diaz, B. Invadopodia Detection and Gelatin Degradation Assay. *Bio-Protocol* **2013**, *3*, e997. <https://doi.org/10.21769/BioProtoc.997>.
27. Agarwal, S.; Gertler, F.B.; Balsamo, M.; et al. Quantitative assessment of invasive mena isoforms (Mena^{calc}) as an independent prognostic marker in breast cancer. *Breast Cancer Res.* **2012**, *14*, R124.
28. Wang, Z.; Zhang, H.; Hou, J.; et al. Clinical implications of β -catenin protein expression in breast cancer. *Int. J. Clin. Exp. Pathol.* **2015**, *8*, 14989.
29. Lin, S.-Y.; Xia, W.; Wang, J.C.; et al. β -catenin, a novel prognostic marker for breast cancer: Its roles in cyclin D1 expression and cancer progression. *Proc. Natl. Acad. Sci. USA* **2000**, *97*, 4262–4266.
30. Mendes, O.; Kim, H.-T.; Stoica, G. Expression of MMP2, MMP9 and MMP3 in breast cancer brain metastasis in a rat model. *Clin. Exp. Metastasis* **2005**, *22*, 237–246.
31. Yousef, E.M.; Tahir, M.R.; St-Pierre, Y.; et al. MMP-9 expression varies according to molecular subtypes of breast cancer. *BMC Cancer* **2014**, *14*, 609.
32. La Rocca, G.; Pucci-Minafra, I.; Marrazzo, A.; et al. Zymographic detection and clinical correlations of MMP-2 and MMP-9 in breast cancer sera. *Br. J. Cancer* **2004**, *90*, 1414–1421.
33. Joseph, C.; Alsaleem, M.; Orah, N.; et al. Elevated MMP9 expression in breast cancer is a predictor of shorter patient survival. *Breast Cancer Res. Treat.* **2020**, *182*, 267–282.
34. Owyong, M.; Chou, J.; van den Bijgaart, R.J.; et al. MMP9 modulates the metastatic cascade and immune landscape for breast cancer anti-metastatic therapy. *Life Sci. Alliance* **2019**, *2*, e201800226.
35. Mendes, O.; Kim, H.-T.; Lungu, G.; et al. MMP2 role in breast cancer brain metastasis development and its regulation by TIMP2 and ERK1/2. *Clin. Exp. Metastasis* **2007**, *24*, 341–351.
36. Nakopoulou, L.; Tsirmpa, I.; Alexandrou, P.; et al. MMP-2 protein in invasive breast cancer and the impact of MMP-2/TIMP-2 phenotype on overall survival. *Breast Cancer Res. Treat.* **2003**, *77*, 145–155.
37. Baranwal, S.; Alahari, S.K. Molecular mechanisms controlling E-cadherin expression in breast cancer. *Biochem. Biophys. Res. Commun.* **2009**, *384*, 6–11.
38. Singhai, R.; Patil, V.W.; Jaiswal, S.R.; et al. E-Cadherin as a diagnostic biomarker in breast cancer. *N. Am. J. Med. Sci.* **2011**, *3*, 227.
39. Kleer, C.G.; van Golen, K.L.; Braun, T.; et al. Persistent E-cadherin expression in inflammatory breast cancer. *Mod. Pathol.* **2001**, *14*, 458–464.
40. Jiang, P.; Enomoto, A.; Takahashi, M. Cell biology of the movement of breast cancer cells: Intracellular signalling and the actin cytoskeleton. *Cancer Lett.* **2009**, *284*, 122–130.
41. Pollard, T.D.; Borisy, G.G. Cellular motility driven by assembly and disassembly of actin filaments. *Cell* **2003**, *112*, 453–465.
42. Roussos, E.T.; Goswami, S.; Balsamo, M.; et al. Mena invasive (Mena INV) and Mena11a isoforms play distinct roles in breast cancer cell cohesion and association with TMEM. *Clin. Exp. Metastasis* **2011**, *28*, 515–527.
43. Oudin, M.J.; Barbier, L.; Schäfer, C.; et al. MENA confers resistance to paclitaxel in triple-negative breast cancer. *Mol. Cancer Ther.* **2017**, *16*, 143–155.
44. Martin, T.A.; Mansel, R.E.; Jiang, W.G. Loss of occludin leads to the progression of human breast cancer. *Int. J. Mol. Med.* **2010**, *26*, 723–734. https://doi.org/10.3892/ijmm_00000519.

45. Moses, H.; Barcellos-Hoff, M.H. TGF- β biology in mammary development and breast cancer. *Cold Spring Harb. Perspect. Biol.* **2011**, 3, a003277.
46. Qiu, L.-X.; Yao, L.; Mao, C.; et al. TGFB1 L10P polymorphism is associated with breast cancer susceptibility: Evidence from a meta-analysis involving 47,817 subjects. *Breast Cancer Res. Treat.* **2010**, 123, 563–567.
47. Scollen, S.; Luccarini, C.; Baynes, C.; et al. TGF- β signaling pathway and breast cancer susceptibility. *Cancer Epidemiol. Prev. Biomark.* **2011**, 20, 1112–1119.
48. Bergom, C.; Gao, C.; Newman, P.J. Mechanisms of PECAM-1-mediated cytoprotection and implications for cancer cell survival. *Leuk. Lymphoma* **2005**, 46, 1409–1421.
49. Cao, G.; O'Brien, C.D.; Zhou, Z.; et al. Involvement of human PECAM-1 in angiogenesis and in vitro endothelial cell migration. *Am. J. Physiol.-Cell Physiol.* **2002**, 282, C1181–C1190.
50. Rydén, L.; Linderholm, B.; Nielsen, N.H.; et al. Tumor specific VEGF-A and VEGFR2/KDR protein are co-expressed in breast cancer. *Breast Cancer Res. Treat.* **2003**, 82, 147–154.
51. Yan, J.-D.; Liu, Y.; Zhang, Z.-Y.; et al. Expression and prognostic significance of VEGFR-2 in breast cancer. *Pathol.-Res. Pract.* **2015**, 211, 539–543.
52. Zhao, J.; Yang, C.; Guo, S.; et al. GM130 regulates epithelial-to-mesenchymal transition and invasion of gastric cancer cells via snail. *Int. J. Clin. Exp. Pathol.* **2015**, 8, 10784.
53. Foley, J.; Nickerson, N.K.; Nam, S.; et al. EGFR signaling in breast cancer: Bad to the bone. *Semin. Cell Dev. Biol.* **2010**, 21, 951–960.
54. Maennling, A.E.; Tur, M.K.; Niebert, M.; et al. Molecular targeting therapy against EGFR family in breast cancer: Progress and future potentials. *Cancers* **2019**, 11, 1826.
55. Ali, R.; Wendt, M.K. The paradoxical functions of EGFR during breast cancer progression. *Signal Transduct. Target. Ther.* **2017**, 2, 16042.
56. Ham, S.A.; Yoo, T.; Lee, W.J.; et al. ADAMTS1-mediated targeting of TSP-1 by PPAR δ suppresses migration and invasion of breast cancer cells. *Oncotarget* **2017**, 8, 94091.
57. Tyan, S.-W.; Hsu, C.-H.; Peng, K.-L.; et al. Breast cancer cells induce stromal fibroblasts to secrete ADAMTS1 for cancer invasion through an epigenetic change. *PLoS ONE* **2012**, 7, e35128.
58. Tan, I.A.; Frewin, K.; Ricciardelli, C.; et al. ADAMTS1 promotes adhesion to extracellular matrix proteins and predicts prognosis in early stage breast cancer patients. *Cell Physiol Biochem.* **2019**, 52, 1553–1568.
59. Yang, C.; He, P.; Liu, Y.; et al. Down-regulation of CEACAM1 in breast cancer. *Acta Biochim. Biophys. Sin.* **2015**, 47, 788–794.
60. Wang, J.-L.; Sun, S.-Z.; Qu, X.; et al. Clinicopathological significance of CEACAM1 gene expression in breast cancer. *Chin. J. Physiol.* **2011**, 54, 332–338.
61. Yang, C.; He, P.; Liu, Y.; et al. Assay of serum CEACAM1 as a potential biomarker for breast cancer. *Clin. Chim. Acta* **2015**, 450, 277–281.
62. Bamberger, A.-M.; Kappes, H.; Methner, C.; et al. Expression of the adhesion molecule CEACAM1 (CD66a, BGP, C-CAM) in breast cancer is associated with the expression of the tumor-suppressor genes Rb, Rb2, and p27. *Virchows Arch.* **2002**, 440, 139–144.
63. Sorlie, T.; Perou, C.M.; Tibshirani, R.; et al. Gene expression patterns of breast carcinomas distinguish tumor subclasses with clinical implications. *Proc. Natl. Acad. Sci. USA* **2001**, 98, 10869–10874. <https://doi.org/10.1073/pnas.191367098>.
64. Raza, M.; Prasad, P.; Gupta, P.; et al. Perspectives on the role of brain cellular players in cancer-associated brain metastasis: Translational approach to understand molecular mechanism of tumor progression. *Cancer Metastasis Rev.* **2018**, 37, 791–804. <https://doi.org/10.1007/s10555-018-9766-5>.
65. Zhou, W.; Slingerland, J.M. Links between oestrogen receptor activation and proteolysis: Relevance to hormone-regulated cancer therapy. *Nat. Rev. Cancer* **2014**, 14, 26–38.
66. Group, E.B.C.T.C. Tamoxifen for early breast cancer: An overview of the randomised trials. Early Breast Cancer Trialists' Collaborative Group. *Lancet* **1998**, 351, 1451–1467. [https://doi.org/10.1016/S0140-6736\(97\)11423-4](https://doi.org/10.1016/S0140-6736(97)11423-4).
67. Romond, E.H.; Perez, E.A.; Bryant, J.; et al. Trastuzumab plus adjuvant chemotherapy for operable HER2-positive breast cancer. *N. Engl. J. Med.* **2005**, 353, 1673–1684. <https://doi.org/10.1056/NEJMoa052122>.
68. Stringer-Reasor, E.M.; May, J.E.; Olariu, E.; et al. An open-label, pilot study of veliparib and lapatinib in patients with metastatic, triple-negative breast cancer. *Breast Cancer Res.* **2021**, 23, 30. <https://doi.org/10.1186/s13058-021-01408-9>.
69. Luque-Cabal, M.; Garcia-Teijido, P.; Fernandez-Perez, Y.; et al. Mechanisms Behind the Resistance to Trastuzumab in HER2-Amplified Breast Cancer and Strategies to Overcome It. *Clin. Med. Insights. Oncol.* **2016**, 10, 21–30. <https://doi.org/10.4137/cmo.s34537>.
70. Palethorpe, H.M.; Smith, E. Bacopasides I and II Act in Synergy to Inhibit the Growth, Migration and Invasion of Breast Cancer Cell Lines. *Molecules* **2019**, 24, 3539. <https://doi.org/10.3390/molecules24193539>.

71. Lehmann, B.D.; Bauer, J.A.; Chen, X.; et al. Identification of human triple-negative breast cancer subtypes and preclinical models for selection of targeted therapies. *J. Clin. Investig.* **2011**, *121*, 2750–2767. <https://doi.org/10.1172/jci45014>.
72. Yersal, O.; Barutca, S. Biological subtypes of breast cancer: Prognostic and therapeutic implications. *World J. Clin. Oncol.* **2014**, *5*, 412–424. <https://doi.org/10.5306/wjco.v5.i3.412>.
73. Lebert, J.M.; Lester, R.; Powell, E.; et al. Advances in the systemic treatment of triple-negative breast cancer. *Curr. Oncol.* **2018**, *25*, S142–S150. <https://doi.org/10.3747/co.25.3954>.
74. DeMichele, A.; Yee, D.; Esserman, L. Mechanisms of Resistance to Neoadjuvant Chemotherapy in Breast Cancer. *N. Engl. J. Med.* **2017**, *377*, 2287–2289. <https://doi.org/10.1056/NEJMcibr1711545>.
75. Lin, N.U.; Claus, E.; Sohl, J.; et al. Sites of distant recurrence and clinical outcomes in patients with metastatic triple-negative breast cancer: High incidence of central nervous system metastases. *Cancer* **2008**, *113*, 2638–2645. <https://doi.org/10.1002/cncr.23930>.
76. Kassam, F.; Enright, K.; Dent, R.; et al. Survival outcomes for patients with metastatic triple-negative breast cancer: Implications for clinical practice and trial design. *Clin. Breast Cancer* **2009**, *9*, 29–33. <https://doi.org/10.3816/CBC.2009.n.005>.
77. Agulnik, M.; Cohen, E.W.; Cohen, R.B.; et al. Phase II study of lapatinib in recurrent or metastatic epidermal growth factor receptor and/or erbB2 expressing adenoid cystic carcinoma and non adenoid cystic carcinoma malignant tumors of the salivary glands. *J. Clin. Oncol. Off. J. Am. Soc. Clin. Oncol.* **2007**, *25*, 3978–3984. <https://doi.org/10.1200/jco.2007.11.8612>.
78. Harrington, K.J.; El-Hariry, I.A.; Holford, C.S.; et al. Phase I study of lapatinib in combination with chemoradiation in patients with locally advanced squamous cell carcinoma of the head and neck. *J. Clin. Oncol. Off. J. Am. Soc. Clin. Oncol.* **2009**, *27*, 1100–1107. <https://doi.org/10.1200/jco.2008.17.5349>.
79. Polychronis, A.; Sinnett, H.D.; Hadjiminis, D.; et al. Preoperative gefitinib versus gefitinib and anastrozole in postmenopausal patients with oestrogen-receptor positive and epidermal-growth-factor-receptor-positive primary breast cancer: A double-blind placebo-controlled phase II randomised trial. *Lancet. Oncol.* **2005**, *6*, 383–391. [https://doi.org/10.1016/s1470-2045\(05\)70176-5](https://doi.org/10.1016/s1470-2045(05)70176-5).
80. Arteaga, C.L.; O'Neill, A.; Moulder, S.L.; et al. A phase I-II study of combined blockade of the ErbB receptor network with trastuzumab and gefitinib in patients with HER2 (ErbB2)-overexpressing metastatic breast cancer. *Clin. Cancer Res. Off. J. Am. Assoc. Cancer Res.* **2008**, *14*, 6277–6283. <https://doi.org/10.1158/1078-0432.ccr-08-0482>.
81. Rexer, B.N.; Engelman, J.A.; Arteaga, C.L. Overcoming resistance to tyrosine kinase inhibitors: Lessons learned from cancer cells treated with EGFR antagonists. *Cell Cycle* **2009**, *8*, 18–22. <https://doi.org/10.4161/cc.8.1.7324>.
82. Cristofanilli, M.; Valero, V.; Mangalik, A.; et al. Phase II, randomized trial to compare anastrozole combined with gefitinib or placebo in postmenopausal women with hormone receptor-positive metastatic breast cancer. *Clin. Cancer Res. Off. J. Am. Assoc. Cancer Res.* **2010**, *16*, 1904–1914. <https://doi.org/10.1158/1078-0432.ccr-09-2282>.
83. Liu, C.Y.; Hu, M.H.; Hsu, C.J.; et al. Lapatinib inhibits CIP2A/PP2A/p-Akt signaling and induces apoptosis in triple negative breast cancer cells. *Oncotarget* **2016**, *7*, 9135–9149. <https://doi.org/10.18632/oncotarget.7035>.
84. Liu, Z.; Fusi, A.; Schmittel, A.; et al. Eradication of EGFR-positive circulating tumor cells and objective tumor response with lapatinib and capecitabine. *Cancer Biol. Ther.* **2010**, *10*, 860–864. <https://doi.org/10.4161/cbt.10.9.13323>.
85. Takahashi, K.; Tanaka, M.; Inagaki, A.; et al. Establishment of a 5-fluorouracil-resistant triple-negative breast cancer cell line. *Int. J. Oncol.* **2013**, *43*, 1985–1991. <https://doi.org/10.3892/ijo.2013.2135>.
86. Witzel, I.; Oliveira-Ferrer, L.; Pantel, K.; et al. Breast cancer brain metastases: Biology and new clinical perspectives. *Breast Cancer Res.* **2016**, *18*, 8. <https://doi.org/10.1186/s13058-015-0665-1>.
87. Ma, S.; Dielschneider, R.F.; Henson, E.S.; et al. Ferroptosis and autophagy induced cell death occur independently after siramesine and lapatinib treatment in breast cancer cells. *PLoS ONE* **2017**, *12*, e0182921. <https://doi.org/10.1371/journal.pone.0182921>.
88. Guan, M.; Tong, Y.; Guan, M.; et al. Lapatinib Inhibits Breast Cancer Cell Proliferation by Influencing PKM2 Expression. *Technol. Cancer Res. Treat.* **2018**, *17*, 1533034617749418. <https://doi.org/10.1177/1533034617749418>.